Self-Excited Noise Generation from Laminar Methane/Air Premixed Flames in Thin Annular Jets

K. N. Kim, J. H. Joung, S. H. Jin and S. H. Chung*

School of Mechanical and Aerospace Engineering,
Seoul National University,
Seoul, 151-742, Korea
shchung@snu.ac.kr

Abstract: Self-excited noise generation from laminar flames in thin annular jets of methane/air premixture has been investigated experimentally. Various flames were observed in this flow configuration, including conical shape flames, ring shape flames, steady crown shape flames, and oscillating crown shape flames. Self-excited noise with the total sound pressure level of about 70dB was generated from the oscillating crown shape flames for the equivalence ratio larger than 0.95. Sound pressure and CH* chemiluminescence were measured by using a microphone and a photomultiplier tube. The frequency of generated noise was measured as functions of equivalence ratio and premixture velocity. A frequency doubling phenomena have also been observed. The flame shape during flame oscillation was reconfirmed by a synchronized PIV experiment. The velocity and pressure field were obtained from PIV. The minimum pressure was formed near the edge of flame representing circulation. By comparing the results of sound pressure, flame luminosity and PIV, the noise source can be attributed to the flame front fluctuation near the edge of the oscillating crown-shape flames.

Keywords: Annular Jet, Laminar Premixed Flame, Sound Pressure, flame luminosity, PIV

1. Introduction

Recent demands for high combustion loads and stringent emission requirements frequently induce combustion instabilities and oscillations. Since these are undesirable sources of noise and sometimes cause disastrous destruction of combustion equipments, an active control of combustion instabilities/oscillations becomes one of the key interests in combustion researches. In order to develop effective control technologies, it is required to understand the mechanisms and the influencing factors governing combustion instabilities and oscillations.

Previous studies on unsteady combustion instabilities have been frequently focused on propulsion systems such as rocket motors [1-3], jet engine afterburners [4, 5], and ramjets [6-9]. These phenomena are coupled by complex, feedback-type interactions between flow, acoustics, and combustion processes. Recently, attentions are focused on the source of combustion noise by investigating relatively simple and well-defined flow geometries. In this regards, the investigation on laminar jet flames impinged on a cool plate showed that the source of sound generation is from periodic sudden extinction of large portion of the flame interacted with the cool plate [10]. The response of burner-stabilized flat flames to acoustic velocity perturbations has also been investigated numerically and analytically [11]. These studies utilized the forcing of the flow fields by acoustic speakers. While, studies on self-excited combustion noise generation in simple laminar flow geometries are rather limited.

In practical combustion devices, combustion proceeds in turbulent mode, where the combustion characteristics depend sensitively on length scales of turbulence. In this regard, thin annular jet flames of laminar premixed methane/air mixtures have been investigated with the annulus width in the order of 1 mm. This type of flow geometry has been investigated previously in terms of flame stabilization [12]. Depending on the equivalence ratio and jet velocity, self-excited combustion noises have been generated [13]. The present study focused on the self-excited noise generation in the burner, especially the regimes and overall characteristics of noise generation.
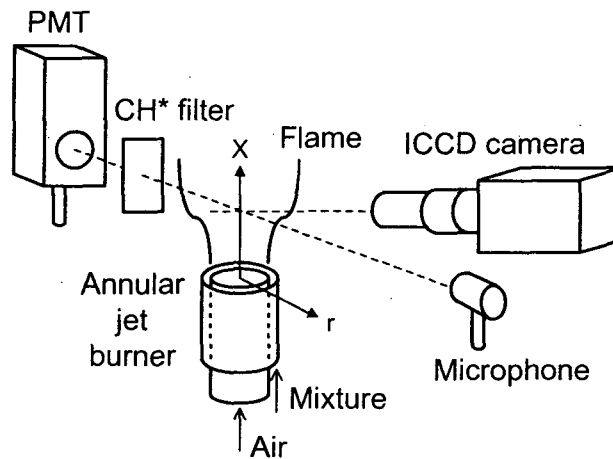
2. Experiment

Fig. 1 Schematics of experimental setup

The apparatus consisted of an annular jet burner and flow controllers, a visualization setup, a sound pressure measurement system, and a PIV system. The annular jet burner, as schematically shown in Fig. 1, was composed of double concentric tubes, which were made of brass. The inner tube is 400 mm long with i.d. 10.1 mm and o.d. 10.9 mm. The outer tube was 300 mm long with i.d. 12.8 mm and o.d. 13.8 mm. The annular slit width was 0.95 mm and the exit area of the annulus was $A = 35.37$ mm^2. The concentricity of the two tubes was maintained by a set of screws installed at the upstream of the outer tube.

The fuel was chemically-pure grade (> 99.95 %) methane. Compressed air was used as an oxidizer. Fuel and air were metered by using mass flow controllers, which were calibrated with a wet-test gas meter. A honeycomb and glass beads were installed in the annulus to ensure premixing. The fuel/air mixture was supplied through the annulus and the air was supplied through th e inner tube. The equivalence ratio and velocities of the premixture and air were the parameters in observing the flame behavior.

The chemiluminescence signals from CH* radicals were measured using a photomultiplier tube (PMT) through a band-pass filter (431 nm, FWHM = 5 nm). The PMT was positioned at the radial location of $r = 27$ cm and the axial location of $X = 3$ cm from the center of the nozzle exit. The signal was sampled at 8.19 kHz. The flame images were taken with an ICCD camera (Princeton Instruments).

For the measurement of sound pressure, a microphone (4189, B&K) was placed at $r = 31$ cm and $X = 3$ cm. Instantaneous sound pressure signals were recorded at 8.19 kHz with the spectral resolution of 0.5 Hz.
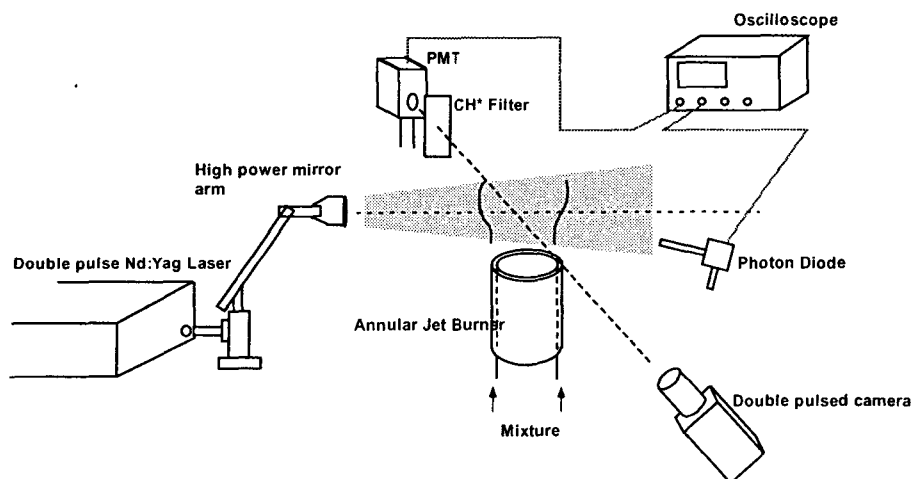

Fig. 2 Experimental setup for PIV

The PIV system consisted of a double pulse Nd:Yag laser (Spectra-Physics, PIV 200) having 10 Hz repetition rate with high power mirror arm, and a double pulsed camera (Kodak Megaplus ES 1.0) A photo diode, an oscilloscope

(Lecroy 9304A) and PMT with a band pass filter (400 nm, FWHM = 30 nm) were utilized to synchronize the PIV system with a flame luminosity variation from flame oscillation. The experimental setup for PIV measurement with synchronization instrument is shown in Fig. 2.

3. Results and discussion

3.1 Observed flames
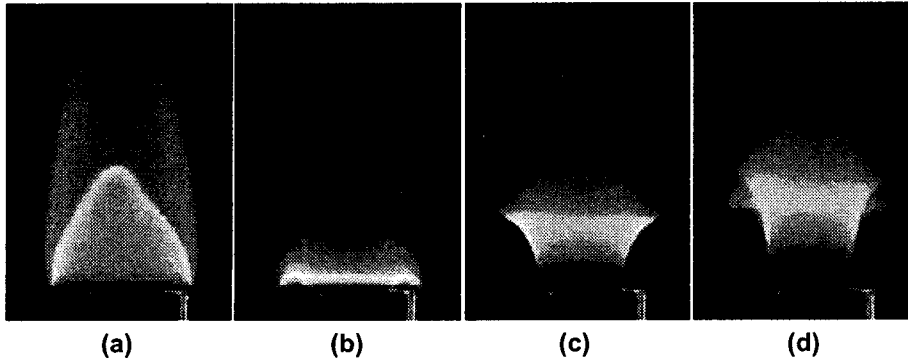

(a)   **(b)**   **(c)**   **(d)**

Fig. 3 Direct photographs of flames in thin annular jet burner; (a) conical shape (ϕ = 1.6, Up = 1.4 m/s), (b) ring shape (1.2, 1.2 m/s), (c) steady crown shape (1.14, 1.8 m/s), and (d) unsteady crown shape (1.14, 2.5 m/s).

Various flames have been observed depending on the equivalence ratio ϕ and mixture velocity U_p. Direct photographs of typical flames are shown in Fig. 3 for the air velocity in the inner tube $U_a = 0$. The Reynolds number is defined as $U_p D_e / v$, where v is the kinetic viscosity and D_e is the effective diameter based on the flow rate, that is, $D_e = (4A/\pi)^{1/2}$. For the experimental conditions of $U_p = 1.0 - 4.0$ m/s, the Reynolds number is in the range of 400 – 1700. Although not shown, the schlieren images confirmed that the flow was laminar in the present experimental range.

For $\phi = 1.6$ and $U_p = 1.4$ m/s (a), the rich premixed flame has a near conical shape with a diffusion flame surrounding it. Note that the flame is attached along the outer rim and is lifted at the inner rim. As U_p increases, the flame becomes elongated and finally blows off. For $\phi = 1.2$ and $U_p = 1.2$ m/s (b), the rich premixed flame had
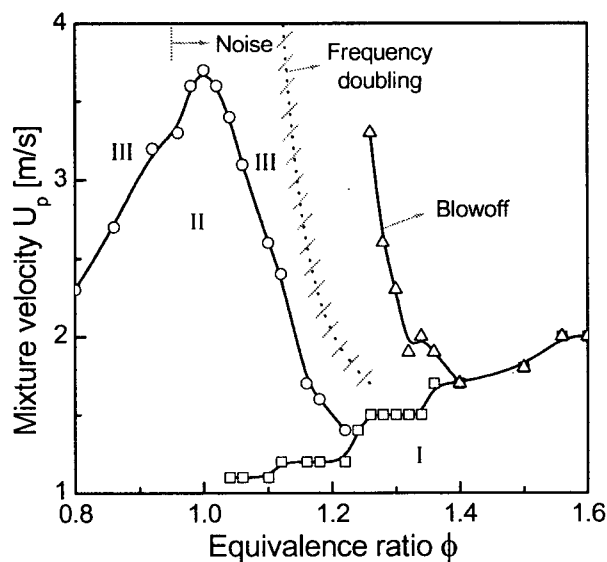

Fig. 4 Regimes of various flames in terms of equivalence ratio and mixture velocity (regime I; ring or conical shape, regime II; steady crown shape, regime III; unsteady crown shape).
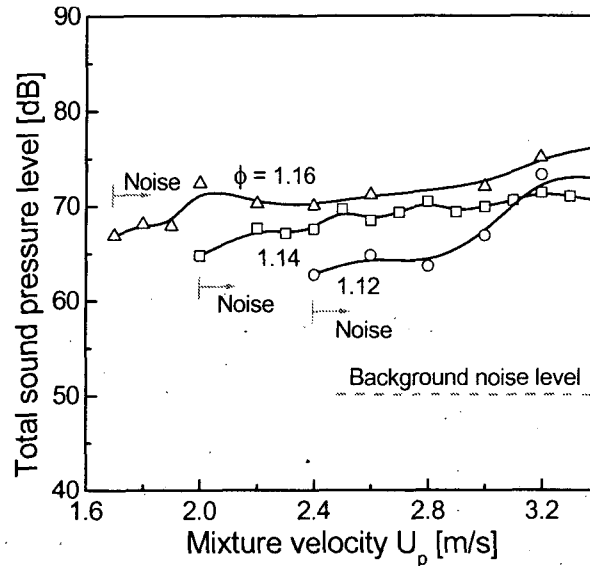
Fig. 5 Sound pressure level as function of mixture velocity at several equivalence ratios.

a ring shape with a diffusion flame surrounding it. The rich premixed flame is attached at both the inner and outer rims. For $\phi = 1.14$ and $U_p = 1.8$ m/s (c), the premixed flame has a crown shape, which is attached at the inner rim and lifted at the outer rim. A diffusion flame is attached near the downstream edge of the crown shaped flame. These three types of flames have been observed previously [13].

With further increasing U_p to 2.5 m/s at $\phi = 1.14$ (d), the flame becomes unsteady having a fluctuation near the downstream edge of the crown shape flame. In such cases, especially for $\phi / 0.95$, appreciable sound noise has been generated having the total sound pressure level of about 70 dB as compared to the background noise level of about 50 dB. This self-excited noise generating flame is the focus of the present study. To examine the possibility of the noise generation by the acoustic resonance in the inner tube, the test has been performed by plugging the inner nozzle exit. The noise generation persisted, suggesting that it is not due to the resonance in the inner tube.

The regime of noise generating flames is shown in Fig. 4 in terms of equivalence ratio and mixture velocity. Regime I is the region for either the ring or conical shape, which has been investigated previously [13]. As U_p increases for $0.8 < \phi < 1.25$, the flame was changed from steady outer lifted flame (regime II) to the oscillating outer lifted flame (regime III). For $1.25 < \phi < 1.4$, the flame undergoes from the ring or conical shape (regime I) to
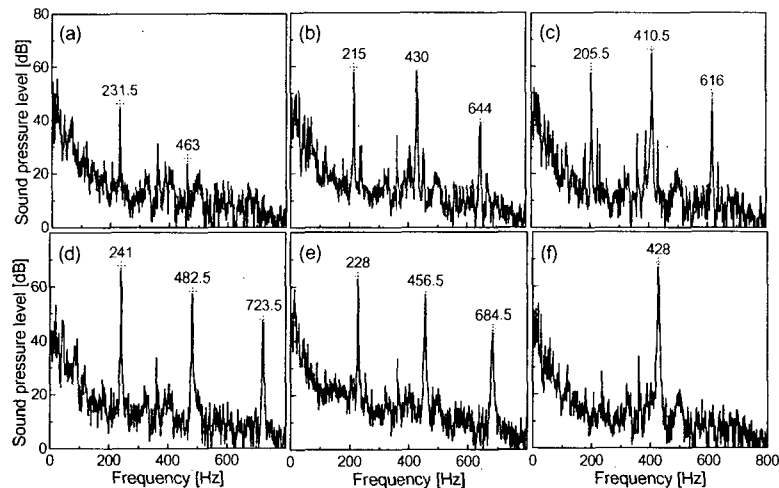

Fig. 6 Sound spectra at various equivalence ratios and mixture velocities; (a) ($\phi = 1.12$, $U_p = 2.6$ m/s), (b) (1.14, 2.6 m/s), (c) (1.16, 2.6 m/s), (d) (1.12, 3.2 m/s), (e) (1.14, 3.2 m/s), and (f) (1.16, 3.2 m/s).
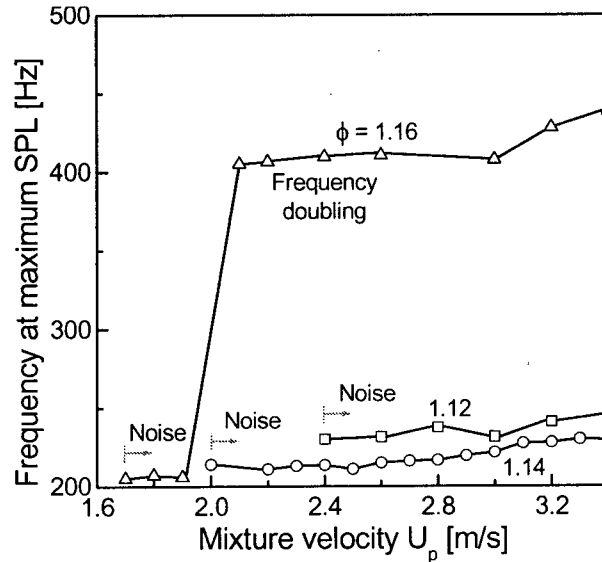
Fig. 7 Frequency at maximum sound pressure level as a function of mixture velocity at several equivalence ratios.

the oscillating outer lifted flame and finally blowoff occurs as U_p increases. For $\phi > 1.4$, the ring shaped flame becomes near conical shape and blowoff occurs as U_p increases. Although not shown in this figure, the flame has either a crown shape or a ring shape for $U_p < 1$ m/s. The frequency doubling behavior in regime III will be discussed later.

3.2 Noise generating flames

The total sound pressure levels of the unsteady crown shape flame for $\phi = 1.12$, 1.14, and 1.16 are shown in Fig. 5. Two points are to be noted. First, the total sound pressure level is reasonably insensitive to the variation in the mixture velocity, even though a slightly increasing trend is observed with U_p. The background noise level marked as the dashed line is about 50 dB. This level is nearly unchanged for both the steady flame cases and the cold jets without having flames. Compared to this level, the total sound pressure level is about 20 dB higher for the
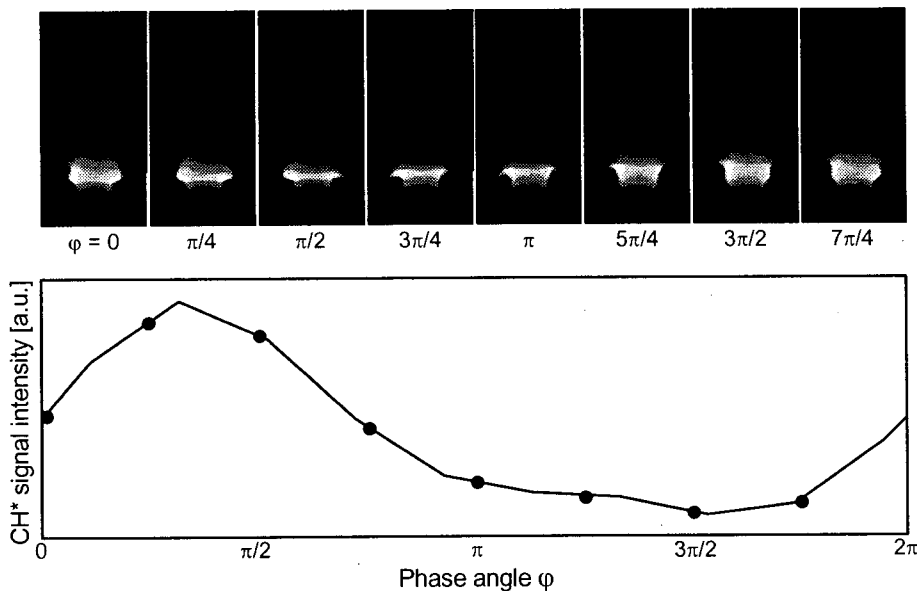

Fig. 8 Variation of flame shape and CH* signal as function of phase angle for $\phi = 1.14$ and $U_p = 2.5$ m/s.
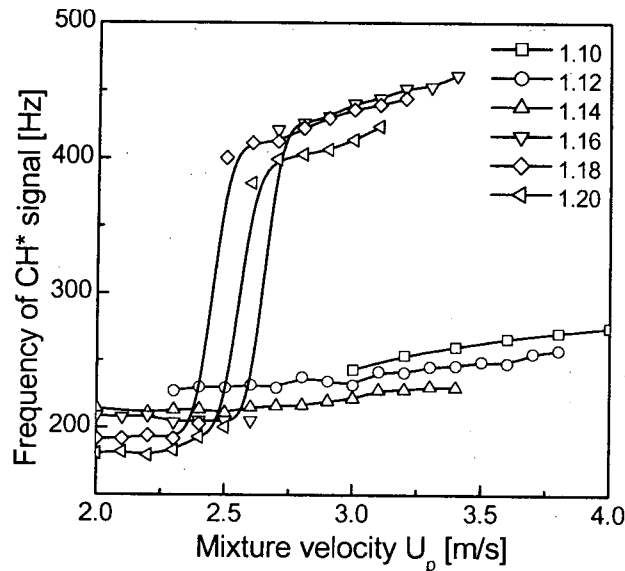
Fig. 9 Peak frequency from FFT of chemiluminescence of CH* as function of mixture velocity at several equivalence ratios.

unsteady crown shape flames. Second point is that the velocity at the onset of noise generation is sensitive to the equivalence ratio.

The noise generation characteristics are further analyzed. The sound pressure level (SPL) in terms of frequency is presented in Fig. 6, demonstrating the spectral distributions at several equivalence ratios (ϕ= 1.12, 1.14, and 1.16) and mixture velocities (U_p = 2.6 and 3.2 m/s). The SPL shows several discrete peaks, which are marked in frequency value. These peaks are imbedded in the background noise level, which generally decreases with frequency. The peaks in the sound spectra are influenced sensitively by the equivalence ratio and mixture velocity. For U_p = 2.6 m/s, the fundamental frequency is 231.5 Hz with its level of about 50 dB for ϕ = 1.12 (a). The fundamental frequency becomes 215 Hz for ϕ = 1.14 (b) with the SPL of about 60 dB. The SPL of the second harmonic at 430 Hz is comparable to the level of the fundamental frequency. For ϕ= 1.16 (c), the SPL at 410.5 Hz becomes higher than that at 205.5 Hz. As the mixture velocity increase to U_p = 3.2 m/s, the SPL of the fundamental frequency at 241 Hz increases up to 68 dB for ϕ= 1.12 (d). For ϕ= 1.14 (e), the SPL of the fundamental frequency at 228 Hz dominates over that of the second harmonic. For ϕ= 1.16 (f), the SPL at 428 Hz mainly remains. Figure 7 shows the frequency of the peak sound pressure level as a function of mixture velocity. The results show the frequency doubling behavior for the unsteady crown shape flames as mixture velocity increases for ϕ= 1.16, and this trend persists for $\phi\langle$ 1.16 for the present experimental range. This point will be further discussed later.

3.3 CH* chemiluminescence and sound pressure

The characteristics of the unsteady crown shape flame are further analyzed. The CH* chemiluminescence signal shows periodic oscillation, as shown in Fig. 8, during one cycle of oscillation. The ICCD images at several phase angles φ are also exhibited corresponding to the unsteady flame shown in Fig. 3d. The CH* signal shows near sinusoidal behavior and the corresponding flame shapes demonstrate a series of flame surface variation, especially near the downstream part of the flame surface. The waist part of the flame surface starts to corrugate, e.g., at φ = 5π/4, amplified, and migrated downstream. The curved flame surface deflected in such a way that a part of the flame surface is pointing upstream, e.g., at the phase angle φ between π/4 and 5π/4, indicating that the flame edge region fluctuates appreciably.

Since the CH* chemiluminescence could reasonably represent the flame-shape variation, the signals are further analyzed at various test conditions. Figure 9 shows the frequencies of CH* chemiluminescence signals in terms of mixture velocity from the fast Fourier transform (FFT) of the CH* signals. The general behavior agrees qualitatively with the frequency of sound pressure level shown in Fig. 7, in terms of the variation in frequency with equivalence ratio and mixture velocity. However, note that the premixture velocity at the onset of frequency doubling $U_{p,c}$ is shifted toward higher value, e.g., $U_{p,c} \approx$ 2.1 m/s from the sound pressure in Fig. 7, while $U_{p,c} \approx$ 2.7 m/s from the CH* in Fig. 9 for ϕ= 1.16. This can be attributed to the FFT behaviors of the sound and CH* signals. The audible sound could clearly distinguish the frequency doubling through the change in the pitch of noise. This
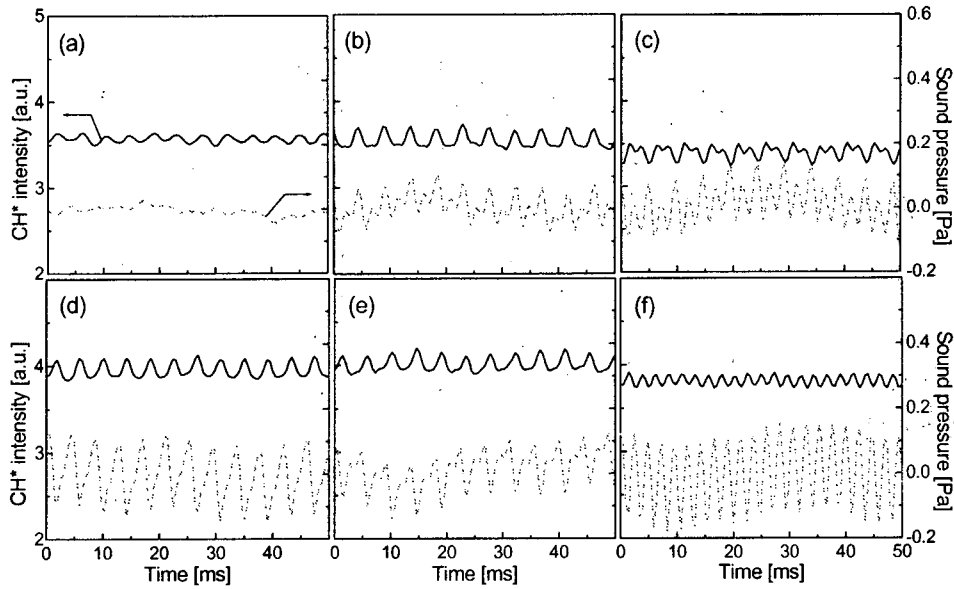
Fig. 10 Comparison of CH* chemiluminescence and sound pressure with time;
(a) (ϕ = 1.12, U_p = 2.6 m/s), (b) (1.14, 2.6 m/s), (c) (1.16, 2.6 m/s),
(d) (1.12, 3.2 m/s), (e) (1.14, 3.2 m/s), and (f) (1.16, 3.2 m/s).

judgement is found to be closely related to the change in the sound pressure level. The boundary of the frequency doubling from the audible noise is marked in Fig. 4 as the dotted line.

Variations of sound pressure and CH* signal with time is compared in Fig. 10 at several combinations of equivalence ratio and mixture velocity. Both signals fluctuate with time. The case (a) shows periodic behavior for the CH* chemiluminescence and the case (b - e) clearly shows frequency doubling behavior. The case (f) again shows periodic behavior, but with higher frequency. These behaviors agree well with those of the peaks in the sound spectra shown in Fig. 6. The behavior of sound pressure closely resembles that of the CH* chemiluminescence.
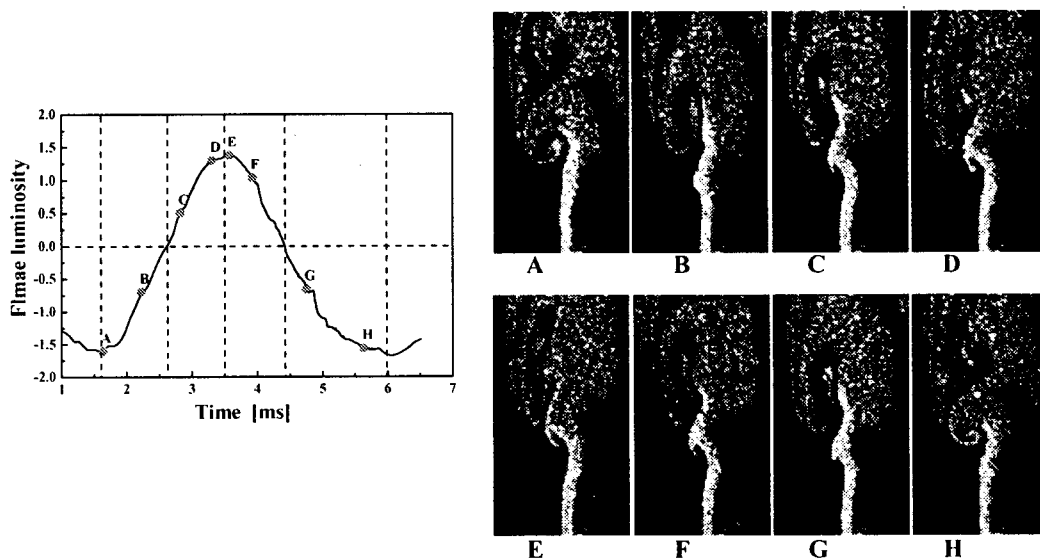

Figure 11. The images of particle image velocitimetry with time for ϕ = 1.18, Up = 2.7 m/s
(The images taken at each of period are gathered in a single period)
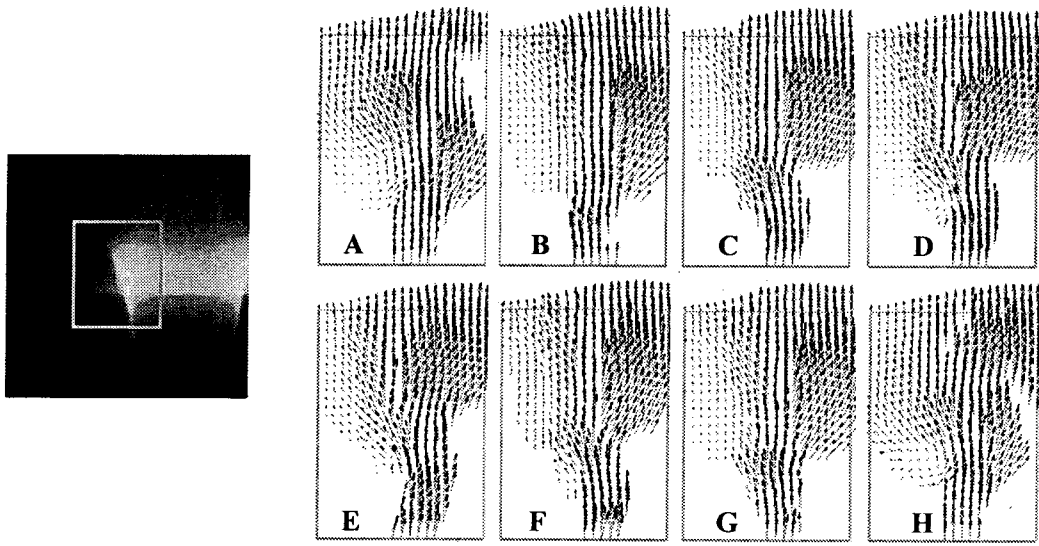
−153−

Fig. 12 The direct photograph of flame and the velocity fields obtained from PIV measurement at each of phase during fluctuation when ϕ = 1.14, U_p = 2.7 m/s

The characteristics of the unsteady crown-shape flame with the oscillation frequency of 220Hz are further analyzed with the synchronized PIV. The time interval between two laser pulses was adjusted to 50 μs. The PIV measurements were conducted at several phases. Figure 11 represents the phases of PIV and the particle images at each phase when ϕ = 1.16, and U_p = 2.7 m/s. The variation of the particle images shows the additional information on flame oscillation. It can be comparable to the ICCD images shown in Fig. 8. The phase of PIV result during oscillation was determined by matching a laser signal with flame luminosity. The signal of laser and flame luminosity were measured simultaneously with a photodiode and a PMT equipped with a band pass filter (400nm, FWHM = 30 nm).
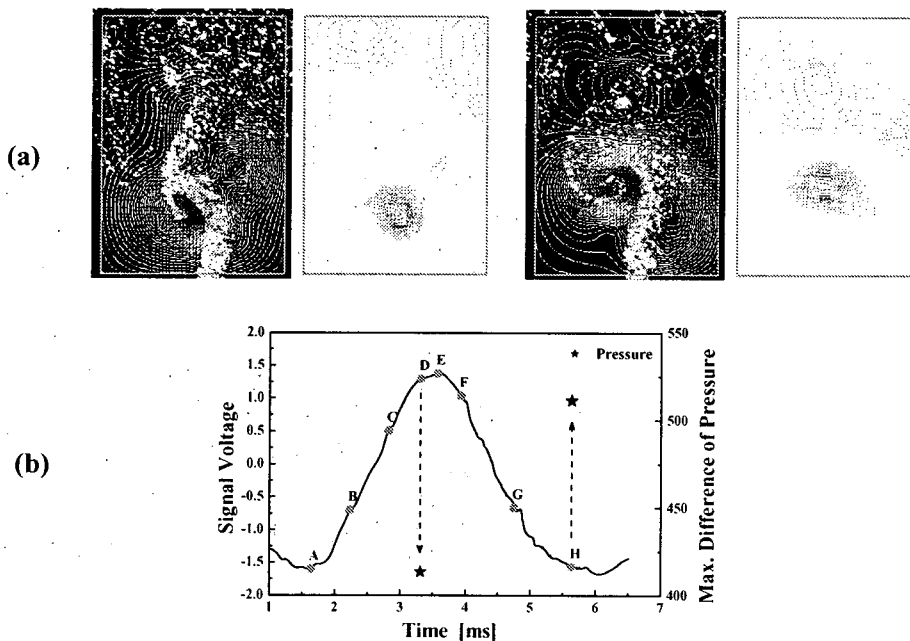

Figure 13. (a) The pressure distribution with particle images and (b) the maximum pressure difference (= P_{max} − P_{min}) in the pressure field at the phases of D and H

Figure 12 shows the time-averaged direct photographs of the oscillating flame and the velocity field in the selected region. The result demonstrates that the formation of vertical structure near the outer edge of the concentric jet, could induce the flame oscillation.

Pressure fields can be calculated from a measured velocity fields at each phase. Representative pressure fields at the phase D ($\sim \pi$) and H ($\sim 2\,\pi$) are shown in Fig. 13 (a). The minimum pressure region is formed where the circulation existed. It can be regarded that the change of pressure difference during flame oscillation generates a noise. The maximum differences in pressure in a pressure field ($\Delta P_{max} = P_{max} - P_{min}$) are shown in Fig. 13(b) together with the flame luminosity variations. The maximum difference of pressure shows the inverse trend with the flame luminosity. It has a maximum (minimum) value when the flame luminosity is minimum (maximum). It implies that the variations of pressure difference created by flame oscillation generates a noise and includes a phase delay of π with the flame luminosity.

4. Conclusion

Premixed methane/air flames in the laminar thin annular jet burner have been studied experimentally to investigate the characteristics of self-excited noise generation. The flame in the annular jets has various flame shapes, including ring shape, near conical shape, crown shape, and oscillating crown shape depending on equivalence ratio, mixture velocity, and air velocity. The regimes of the existence of these flames were identified. Self-excited noise with about 70 dB was generated for the unsteady crown shape flame when the mixture was rich. The frequency of sound pressure depended on the equivalence ratio and mixture velocity. The frequency doubling behavior occurred for richer mixtures. The variation of sound pressure with time showed similar behavior as that of the CH* chemiluminescence. The PIV experiment reconfirmed the variations of flame shape during flame oscillation. The minimum position of a pressure field demonstrates that the source of sound generation is from the flame surface fluctuation near the downstream part of the crown shape flames. By comparing the flame luminosity with maximum pressure difference, it was revealed that they are out-of-phase. Further study is needed in the future to identify the mechanism of flame surface corrugation, the interaction with the diffusion flame surrounding it, and the mechanism of frequency doubling.

5. Acknowledgement

References

1. H. Tsuji, T. Takeno, Tenth Symposium (International) on Combustion, The Combustion Institute, Pittsburgh, 1964, p. 1327.
2. L. Crocco, S. Cheng, Theory of Combustion Instability in Liquid Propellant Rocket Motors, Butterworths Scientific Publications, London, U.K., 1956.
3. B.T. Zinn, E.A. Powell, Thirteenth Symposium (International) on Combustion, The Combustion Institute, Pittsburgh, 1970, p. 491.
4. P.J. Langhorne, J. Fluid Mech. 193 (1988) 417-443.
5. G. Bloxsidge, A. Dowling, P.J. Langhorne, J. Fluid Mech. 193 (1988) 445-473.
6. V. Yang, F.E. Culick, Comb. Sci. and Tech. 45 (1986) 1-25.
7. K.C. Schadow, K.J. Wilson, AIAA Journal 25 (1987) 1164-1170.
8. K.C. Schadow, E. Gutmark, Prog. Energy Combust. Sci. 18 (1992) 117-132.
9. U.G. Hegde, D. Reuter, B.R. Daniel, B.T. Zinn, Comb. Sci. and Tech. 55 (1987) 125-138.
10. T. Schuller, D. Durox, S. Candel, Combust. Flame 128 (2002) 88-110.
11. R. Rock, L.P.H. Goey, L.M.T. Somers, K.R.A.M. Schreel, R. Parchen, Combust. Theory Modelling 6 (2002) 223-242.
12. Z. Shu, S.K. Aggarwal, V.R. Katta, I.K. Puri, Combust. Flame 111 (1997) 276-295.
13. S.J. Kwon, M.S. Cha, M.S. Choi, S.H. Chung, Trans. KSME (B) 24 (2000) 1662-1669.
14. R.B. Price, I.R. Hurle, T.M. Sugden, Twelfth Symposium (International) on Combustion, The Combustion Institute, Pittsburgh, 1968, p. 1093.
15. S. Ducruix, D. Durox, S. Candel, Proceedings of the Combustion Institute, Vol. 28, The Combustion Institute, Pittsburgh, 2000, p. 765